Abdominal Radiology (2019) 44:1033–1043
https://doi.org/10.1007/s00261-018-1871-y

KIDNEYS, URETERS, BLADDER, RETROPERITONEUM

Evaluation of diagnostic accuracy: multidetector CT image noise correction improves specificity of a Gaussian model-based algorithm used for characterization of incidental adrenal nodules

Toshimasa J. Clark[1] · Larson D. Hsu[2] · Daniel Hippe[3] · Sophie Cowan[3] · Jonathan Carnell[3] · Carolyn L. Wang[3]

Published online: 1 January 2019

Abstract

Objectives To investigate whether the histogram analysis method of characterizing adrenal nodules as adenomas is affected by increased noise with modern CT technique, and if an extension that allows for noise correction will improve diagnostic performance.

Materials and methods This is a HIPAA-compliant, IRB-approved retrospective study performed on 58 total patients. The first group of 29 patients had 33 adrenal lesions that were pathology-proven non-adenomas. The second group had 29 patients with 33 pathology-proven or presumed adenomas based on established imaging criteria. The nodules were evaluated using the histogram method, mean attenuation method, and a Gaussian model-based algorithm without (uncorrected Gaussian algorithm) and with correction (corrected Gaussian algorithm) for image noise. Sensitivity, specificity, and accuracy for identifying adenoma were derived.

Results There were no significant differences in identifying adenoma from non-adenoma when using the histogram analysis method and the uncorrected Gaussian algorithm, both of which had low specificities of 42.4% and 47.0%, respectively ($p = 0.30$). Adding noise correction to the Gaussian algorithm resulted in a statistically significant increase in specificity relative to the histogram method (86.4% vs. 42.4%, $p < 0.001$). The corrected Gaussian algorithm improved sensitivity compared to the mean attenuation method (71.2% vs. 54.5%, $p < 0.001$), but had lower specificity (86.4% vs. 100%, $p < 0.001$), and similar overall accuracy (78.8% vs. 77.3%, $p = 0.74$).

Conclusion With modern low-dose CT technique, the specificity scores of the histogram method for discrimination of adrenal adenomas and non-adenomas are lower than with previous higher dose scans. The specificity and accuracy of a histogram-equivalent method can be increased mathematically through image noise correction, and the corrected Gaussian algorithm has improved sensitivity to the mean attenuation with similar accuracy albeit with lower specificity. Although this suggests limited utility for histogram analysis in adrenal nodule characterization, our study demonstrates the potential mathematical application for other noise-dependent CT characterization methods.

Keywords Adrenal nodule · Adrenal adenoma · Histogram analysis · Gaussian algorithm · Noise correction

Introduction

Adrenal nodules are common imaging findings, observed in 4–5% of abdominopelvic CT studies [1]. Diagnosis of an adrenal adenoma based on mean attenuation < 10 HU on noncontrast CT is a common clinical practice, however this method is known to misclassify lipid-poor adrenal adenomas [2]. The enhancement washout technique has been shown to have high accuracy but it involves both contrast administration and additional radiation dose to the patient [3, 4]. To improve diagnostic accuracy without additional contrast or imaging phases, the histogram method was later developed,

Electronic supplementary material The online version of this article (https://doi.org/10.1007/s00261-018-1871-y) contains supplementary material, which is available to authorized users.

✉ Toshimasa J. Clark
toshimasa.clark@ucdenver.edu

Extended author information available on the last page of the article

which relies on detection of intralesional fat as evidenced by negative attenuation pixels. In its original description, the histogram method showed an increase in sensitivity for lipid-poor adenomas relative to the mean attenuation method while maintaining specificity on the order of 88–100%. The histogram method's threshold of 10% negative attenuation pixels in a region of interest was derived from CT studies acquired with 5 mm reconstruction slice thickness and fixed 200 effective mAs [5–10]. However, this method requires post processing at a separate workstation for most PACS, and may be prohibitive to standard workflow. In addition, more modern imaging parameters, including thinner reconstructed slice thickness and automated tube current modulation with typically lower tube currents, can result in increased image noise. Specifically, the increased noise is inversely proportional to the square root of decreased photons received at the detector, resulting in higher observed standard deviations of measured attenuation in a given ROI, which would in turn increase false-positive adenomas. No straightforward method exists through which histograms can be corrected for image noise. With new imaging parameters, dose-optimization strategies, and reconstruction methods involved in low-dose imaging, this renders its applicability unclear [11].

Hsu et al. have described a simpler analysis of the proportion of negative pixels in an adrenal nodule's region of interest (ROI) utilizing only the mean attenuation and standard deviation values, and the mathematical properties of a Gaussian distribution [12]. In essence, one can use this method to mathematically recreate the histogram using only the mean attenuation and standard deviation values obtained by drawing an ROI on any standard reading workstation. This Gaussian algorithm should be equivalent to the histogram method, as both rely on the proportion of negative attenuation voxels in a region of interest, as recently confirmed by Rocha et al. [13]. By mathematically altering the standard deviation used in the Gaussian model-based algorithm (subsequently referred to as *"Gaussian algorithm"*) one can correct for image noise, equivalent to performing a histogram analysis with additional noise correction.

The purpose of our study was to investigate whether the histogram analysis method of characterizing adrenal nodules as adenomas is affected by increased noise with modern CT technique, and if an extension that allows for noise correction will improve diagnostic performance.

Materials and methods

This retrospective study was HIPAA-compliant and IRB-approved, and the requirement for informed consent was waived.

Subjects

Patients were retrospectively identified for inclusion through searching two separate databases, from which an adenoma target cohort and a non-adenoma target cohort were constructed. The adenoma target cohort was established primarily through use of free text search of CT scan reports. CT scan reports from 1/1/1999 through 6/6/2014 were searched using zVision (version 1.4.80, Clario Medical Imaging, Inc., Seattle, WA) with the search terms "adrenal nodule", "non-contrast", and "cancer." The initial query resulted in 175 patients. Eighty-seven patients were excluded initially based on criteria related to the CT scanner parameters during image acquisition (Fig. 1), resulting in an intermediate cohort of 97 nodules in 88 patients. Sixty-seven of these nodules were excluded for secondary factors as per Fig. 1, including exclusion of nodules smaller than 1.4 cm (the smallest non-adenoma in our non-adenoma cohort in order to have a more comparable dataset) and exclusion of nodules with macroscopic calcification or fat. Two nodules with malignant pathology were transferred to the non-adenoma cohort. Five additional nodules identified via the adrenal biopsy database were also included in the adenoma cohort, for a final cohort of 33 adenomas in 29 patients.

The non-adenoma target cohort was established primarily through query of an adrenal nodule biopsy database. Pathology reports from all adrenal nodules biopsied percutaneously under CT guidance at our institution between 9/1/2007 and 3/30/2016 were reviewed, which provided predominately non-adenomas. This initial query resulted in a cohort of 40 nodules in 37 patients. Eight nodules were excluded for factors described in Fig. 1. As previously described, seven nodules were transferred between the adenoma and non-adenoma cohorts, resulting in a net decrease of three nodules in the non-adenoma cohort. In patients with proven non-adenoma pathology, four additional nodules were incidentally detected in the contralateral adrenal gland. These had similar imaging characteristics to the non-adenoma and were subsequently included in that group. The final non-adenoma cohort included 33 nodules in 29 patients. The flow chart in Fig. 1 illustrates the inclusion and exclusion of adrenal nodules from both sources. After exclusions and combining the imaging- and pathology-based data sets, there were 33 non-adenomas from 29 patients (4 bilateral) and 33 adenomas from 29 different patients.

Adrenal nodules were defined as adenomas by imaging size stability for > 12 months (< 10% change in the longest axial diameter), signal dropout on chemical-shift MRI, absolute washout of > 60% or relative washout of > 40% on delayed postcontrast CT, negative FDG uptake with FDG-avid primary neoplasm, or negative for malignancy on biopsy. Figure 2 depicts how each presumed adrenal

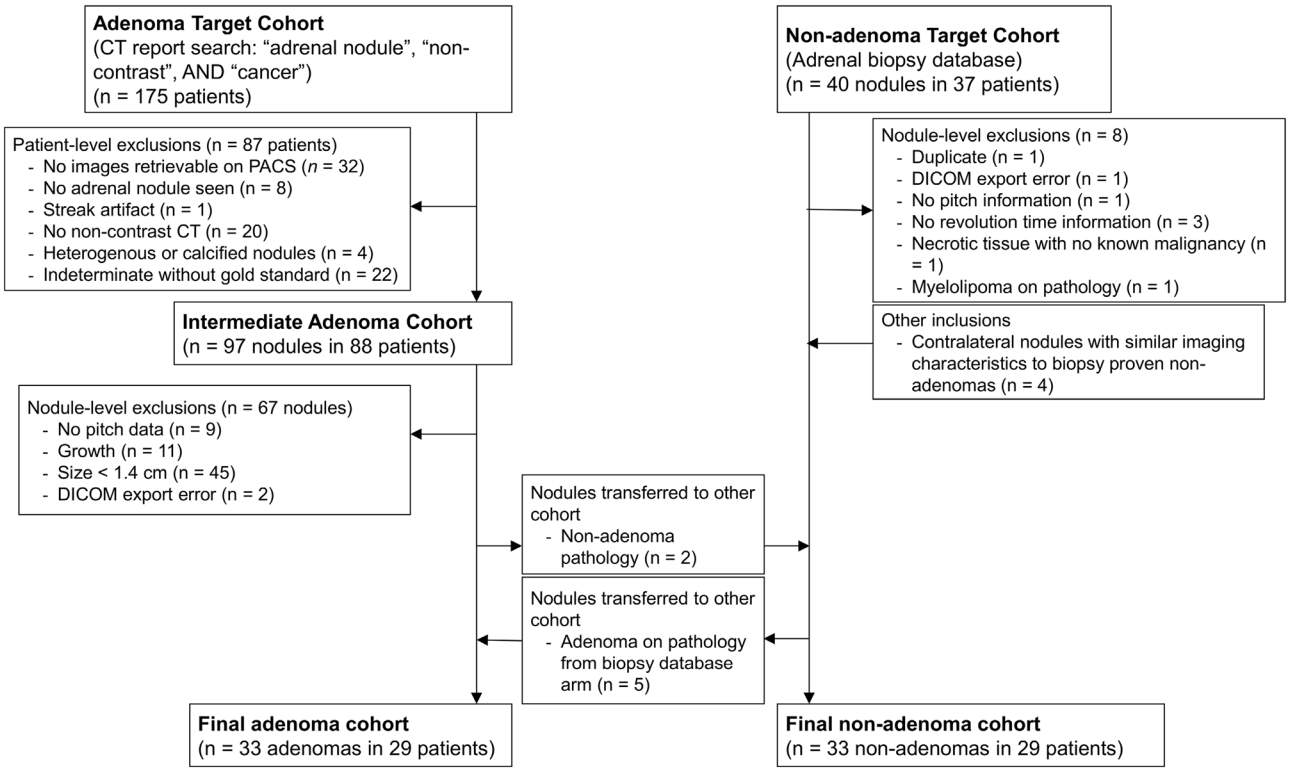

Fig. 1 Patient inclusion and exclusion flowchart

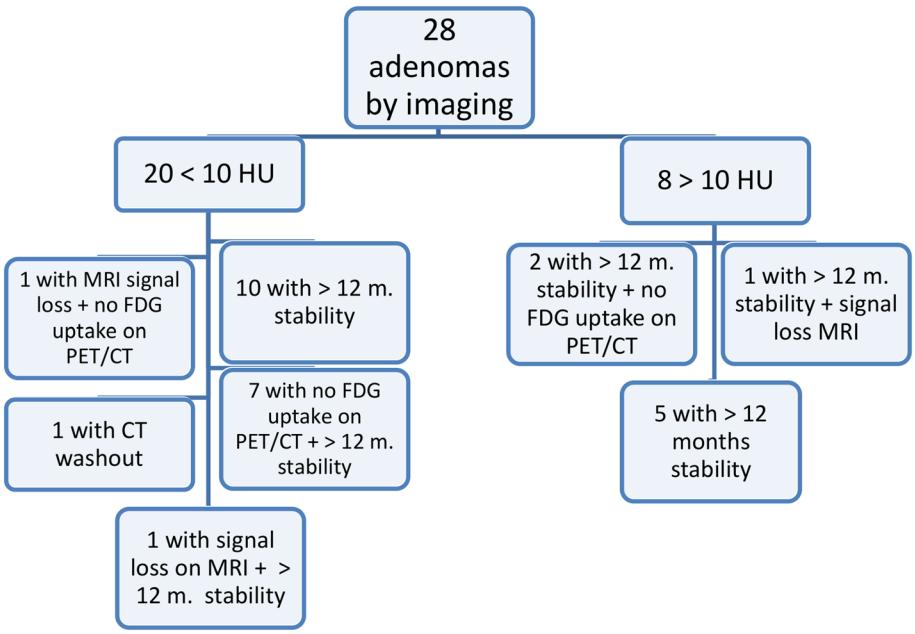

Fig. 2 Characteristics of adenomas defined by imaging

adenoma was characterized. Adrenal nodules were defined as non-adenomas if they had histopathologic assessment positive for malignancy on CT-guided percutaneous adrenal biopsy or surgical resection.

MDCT technique and image analysis

MDCT examinations were acquired by means of GE LightSpeed QXi, GE LightSpeed Ultra, GE VCT 64, GE HD750,

and GE LightSpeed 16 Pro (GE Healthcare, Little Chalfont, UK), and Siemens Definition AS + (Siemens Healtineers, Erlangen, Germany). Image acquisition and reconstruction parameters are summarized in Table 1.

Two independent readers (9 and 2 years of subspecialty experience in abdominal imaging, respectively), blinded to the final outcome, reviewed each index study and measured the nodule's longest axial diameter, mean attenuation, and standard deviation with an ellipsoid ROI > 75% of the adrenal nodule's area. Tube current-time product, reconstruction slice thickness, and pitch factor were recorded using a commercially available PACS interface (Centricity PACS Version 4.0, GE Healthcare, Little Chalfont, UK), and a representative DICOM image was exported. Data were input into an Excel spreadsheet (Office 2013, Microsoft, Inc., Redmond, WA) in which the uncorrected and corrected Gaussian algorithms were implemented:

$$\text{Result} = [\text{Mean attenuation (HU)}] - 1.28 \times [\text{Corrected or uncorrected standard deviation}],$$

where

$$\text{Result} = \text{Upper bound (HU) of the portion of the left tail of a Gaussian distribution that contains 10\% of the total elements in the distribution}$$

$$[\text{Uncorrected standard deviation}] = [\text{Measured standard deviation from ROI}]$$

$$[\text{Corrected standard deviation}] = [\text{Measured standard deviation from ROI}] \times \sqrt{\frac{[\text{slice thickness (mm)}]}{5\,(\text{mm})}} \times \sqrt{\frac{[\text{mA}] \times [\text{rotation time (s)}]}{200\,(\text{mAs}) \times [\text{pitch}]}}$$

The Gaussian algorithm was originally described by Hsu et al. utilizing uncorrected, or measured, standard deviation. Our extension in this work was to modify the standard deviation in order to incorporate noise correction.

The Gaussian algorithm was considered positive for characterization of adrenal adenoma if "Result" was 0 HU or less, which denotes that at least 10% voxels in the ROI measure 0 or less in attenuation [12]. The noise correction is designed to derive the image noise inherent in a study as and if acquired using the original imaging parameters described by Bae and colleagues (5-mm reconstructed slice thickness and 200 effective mAs) via the accepted principle that change in CT noise is proportional to the inverse square of the change in number of photons [5]. This Gaussian algorithm with noise correction is implemented as an Open Source web application at www.raddecisionsupport.com (Fig. 3).

Each exported DICOM image was analyzed using a MATLAB function (R2017a, Mathworks, Inc., Natick, MA) by a third radiologist with 4 years of sub-specialty experience in abdominal imaging, similarly blinded to the outcome. This function implements the mean attenuation, histogram, and corrected and uncorrected Gaussian algorithm methods. The mean attenuation method was considered

Table 1 Study characteristics

Slice thickness (mm)	2.8 (median 2.5, range 2.5–5)
mAs	215 (median 199, range 40–643)
Detector collimation (mm)	0.77 (median 0.625, range 0.625–1.25)
kVp	120 (median 120, range 100–140)
Field of view (cm)	41.8 (median 40.0, range 30.9–70.0)
Rotation time (s)	0.62 (median 0.6, range 0.4–0.91)
Acquisition mode	Helical mode
Pitch	1.34 (median 1.375, range 0.53–1.375)
Reconstruction section thickness (mm)	2.81 (median 2.5, range 2.5–5.0)
Reconstruction section interval (mm)	1.25 (median 0.625, range 0.625–5.0)
Matrix size	512×512
Reconstruction algorithm	Body filter
Convolution kernel	Standard

At the median values of 2.8-mm slice thickness, 215 mAs, 120 kVp, and pitch of 1.34, dose was 45% of that which would be incurred with the original imaging parameters, described by Bae et al., as follows: 5-mm slice thickness, 200 mAs, 120 kVp, and an effective pitch of 1

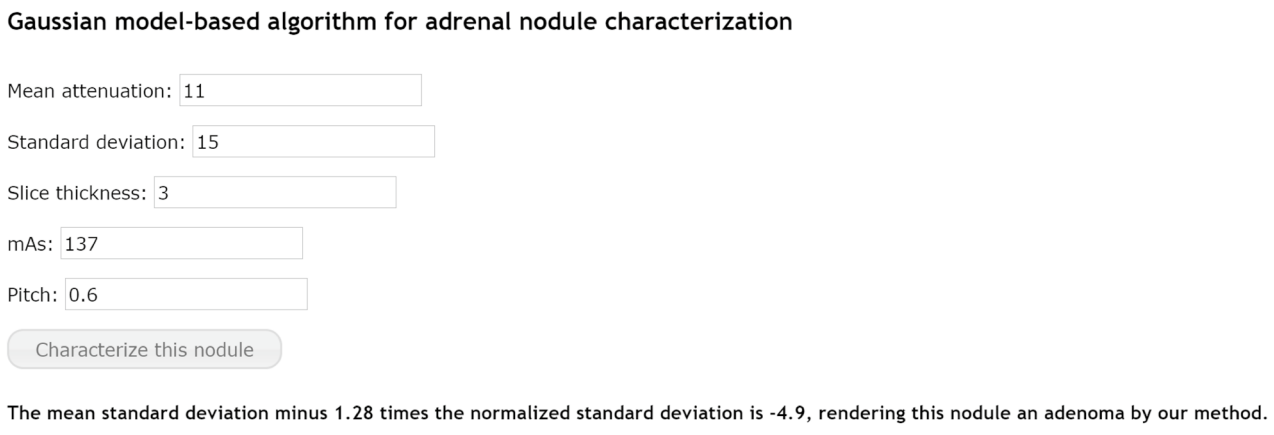

NB: The corrected Gaussian algorithm is:

$$Result = [Mean\ attenuation\ (HU)] - 1.28\ \times\ [Corrected\ or\ uncorrected\ standard\ deviation]$$

, where:

$$Result = Upper\ bound\ (HU)\ of\ the\ portion\ of\ the\ left\ tail\ of\ a\ Gaussian\ distribution\ that\ contains\ 10\%\ of\ the\ total\ elements\ in\ the\ distribution$$

$$[Uncorrected\ standard\ deviation] = [Measured\ standard\ deviation\ from\ ROI]$$

$$[Corrected\ standard\ deviation] = [Measured\ standard\ deviation\ from\ ROI] \times \sqrt{\frac{[slice\ thickness\ (mm)]}{5\ (mm)}} \times \sqrt{\frac{[mA] \times [rotation\ time\ (s)]}{200\ (mAs) \times [pitch]}}$$

The Gaussian algorithm was considered positive for characterization of adrenal adenoma if “Result” was 0 HU or less, which denotes that at least 10% voxels in the ROI measure 0 or less in attenuation. In the example screenshot, “Result” is -4.9 HU, and therefore the nodule in question is considered an adenoma.

Fig. 3 Screenshot of Open Source web application implementing the corrected Gaussian algorithm

positive for adrenal adenoma if attenuation ≤ 10 HU. The histogram analysis method was considered positive for adrenal adenoma if the negative attenuation pixels in the ROI were ≥ 10% of the total.

Statistical methods

Interreader agreement was assessed using the intraclass correlation coefficient (ICC) and Cohen’s kappa. Diagnostic performance for identifying adenomas was summarized for each method using sensitivity (100% × # of true-positive adenomas/# of adenomas), specificity (100% × # true-positive non-adenomas/# of non-adenomas) and overall accuracy. Both readers’ assessments were combined for the analysis (132 total reads of 66 nodules). The nonparametric bootstrap was used to calculate 95% confidence intervals (CIs) and compare methods while accounting for the non-independence among both reads of the same nodule and multiple nodules from the same patient. All statistical calculations were conducted using the statistical computing language R (version 3.1.1; R Foundation for Statistical

Table 2 Primary malignancies identified in non-adenomas

Lung carcinoma[a]	22
Lymphoma	2
Hepatocellular carcinoma	1
Prostate adenocarcinoma	1
Breast carcinoma	1
Angiosarcoma	1
Leiomyosarcoma	1

[a]Four lung cancer patients had bilateral adrenal nodules

Computing, Vienna, Austria). Throughout, two-sided tests were used, with statistical significance defined as $p < 0.05$.

Results

Our final study cohort consisted of 58 nonconsecutive adults (35 men and 23 women) with mean age 64 ± 9.5 years (standard deviation) (range 37–78 years). A total of 66 adrenal nodules were analyzed (8 patients with bilateral nodules), with 33 nodules classified as adenomas and 33 classified as non-adenomas (Fig. 1). The median nodule size was 2.4 cm (interquartile range 1.8–3.5 cm), considering that presumed adenomas < 1.4 cm were excluded, so that both groups had a similar size range. Mean attenuation was 20.1 ± 16.7 HU, and the average standard deviation of attenuation was 24.8 ± 10.4 HU (25.7% had a standard deviation ≥ 30 HU). There was heterogeneity in CT technique (Table 1, but at the median values of 2.8--mm slice thickness, 215 mAs, 120 kVp, and pitch of 1.34, the emitted radiation was 45% of that which would be incurred with the original imaging parameters described by Bae et al. (Table 1). Comparisons of the CT imaging parameters between the non-adenomas and adenomas revealed significantly lower mAs ($p = 0.002$) and mA (median: 209 vs. 453, $p < 0.001$) in the non-adenoma group compared to the adenomas, while the slick thickness ($p = 0.64$), rotation time ($p = 0.37$), and pitch ($p = 0.35$) were not significantly different between the two groups. The non-adenoma group also had a higher uncorrected standard deviation of the attenuation within the nodule than the adenoma group (median: 22.4 vs. 20.4 HU, $p = 0.038$). However, after noise correction of the two standard deviations were similar in the two groups (median: 13.2 vs. 13.5 HU, $p = 0.89$). The most common pathology for non-adenomas was metastasis from lung carcinoma (Table 2).

Diagnostic performance for the histogram, uncorrected Gaussian, corrected Gaussian, and mean attenuation algorithms are summarized in Table 3, with comparisons between methods shown in Table 4. The uncorrected Gaussian algorithm's performance was similar to that of the histogram method, with low specificity for adenomas (47.0% vs. 42.4%, $p = 0.30$) and relatively high sensitivity (86.4% vs.

Table 3 Diagnostic performance for detecting adenoma by different methods

Variable	Histogram method			Uncorrected Gaussian algorithm			Corrected Gaussian algorithm			Mean attenuation < 10 HU		
	No.	Value (%)	(95% CI)	No.	Value (%)	(95% CI)	No.	Value (%)	(95% CI)	No.	Value (%)	(95% CI)
Sensitivity	28/33	84.8	(71.9, 96.8)	57/66	86.4	(73.5, 96.9)	47/66	71.2	(54.8, 87.5)	36/66	54.5	(36.8, 71.4)
Specificity	14/33	42.4	(24.1, 59.5)	31/66	47.0	(28.8, 65.2)	57/66	86.4	(75.0, 95.6)	66/66	100.0	–
Accuracy	42/66	63.6	(50.7, 73.2)	88/132	66.7	(55.5, 77.3)	104/132	78.8	(69.0, 87.7)	102/132	77.3	(68.3, 85.8)

Both readers' assessments were combined for a total of 132 reads

Table 4 Differences in sensitivity and specificity values between different methods

Variable	Uncorrected Gaussian alg. versus histogram method[a]			Corrected Gaussian alg. versus histogram method[a]			Corrected Gaussian alg. versus uncorrected Gaussian alg.[a]		
	Difference	(95% CI)[b]	*p* value	Difference	(95% CI)[b]	*p*-value	Difference	(95% CI)[b]	*p*-value
Sensitivity	1.5	–	> 0.99	−13.6	(−29.0, 0.00)	0.056	−15.2	(−30.0, −1.5)	0.026
Specificity	4.5	(−2.6, 13.2)	0.30	43.9	(26.6, 61.8)	< 0.001	39.4	(23.4, 56.2)	< 0.001
Accuracy	3.0	(−0.8, 7.5)	0.13	15.2	(3.8, 26.5)	0.010	12.1	(0.8, 23.4)	0.035
Variable	Mean attenuation versus histogram method[a]			Mean attenuation versus uncorrected Gaussian alg.[a]			Mean attenuation versus corrected Gaussian alg.[a]		
	Difference	(95% CI)[b]	*p*-value	Difference	(95% CI)[b]	*p*-value	Difference	(95% CI)[b]	*p*-value
Sensitivity	−30.3	(−45.3, −16.2)	<0.001	−31.8	(−47.1, −17.1)	<0.001	−16.7	(−27.9, −6.2)	< 0.001
Specificity	57.6	–	<0.001	53.0	–	<0.001	13.6	–	0.031
Accuracy	13.6	(1.5, 25.8)	0.031	10.6	(−1.5, 23.0)	0.099	−1.5	(−9.2, 6.2)	0.74

[a]Values are difference in performance measures (first method minus second method)

[b]Confidence intervals were not calculated when the performance of either method was 100% or the number of discordant pairs was too low

84.8%, $p > 0.99$). The corrected Gaussian algorithm resulted in statistically significant increases in specificity (86.4% vs. 47.0%, $p < 0.001$) and accuracy (78.8% vs. 66.7%, $p = 0.035$) over the uncorrected Gaussian algorithm, though there was a loss in sensitivity (71.2 vs. 86.4%, $p = 0.026$). The mean attenuation < 10 HU method had significantly lower sensitivity (54.5 vs. 71.2%, difference: −16.7%, $p < 0.001$) and higher specificity than the corrected Gaussian algorithm (100% vs. 86.4%, difference: +13.6%, p = 0.031), but had similar overall accuracy (77.3 vs. 78.8%, difference: −1.5%, 95% CI −9.2 to 6.2%, $p = 0.74$).

Interreader agreement was high with ICC values between 0.80 and 0.99 for mean attenuation and standard deviation of attenuation (measured and corrected) and kappa values between 0.86 and 0.93 for characterization as adenoma or non-adenoma by each method (Online Supplemental Table 1).

Figure 4 depicts the relationship between mean attenuation and negative attenuation percentages for the histogram method, uncorrected Gaussian algorithm, and corrected Gaussian algorithm. The high proportion of non-adenomas (red circles) in the top right quadrant of the uncorrected Gaussian algorithm and histogram method plots indicates false-positive results for these methods. This number of false positives is reduced in the corrected Gaussian algorithm as depicted by the drop of the red circles below the horizontal line. Figure 5 depicts a pathology-proven lung cancer metastasis that was false positive for adenoma by the histogram and uncorrected Gaussian algorithm, but true negative for adenoma by the corrected Gaussian algorithm and the mean

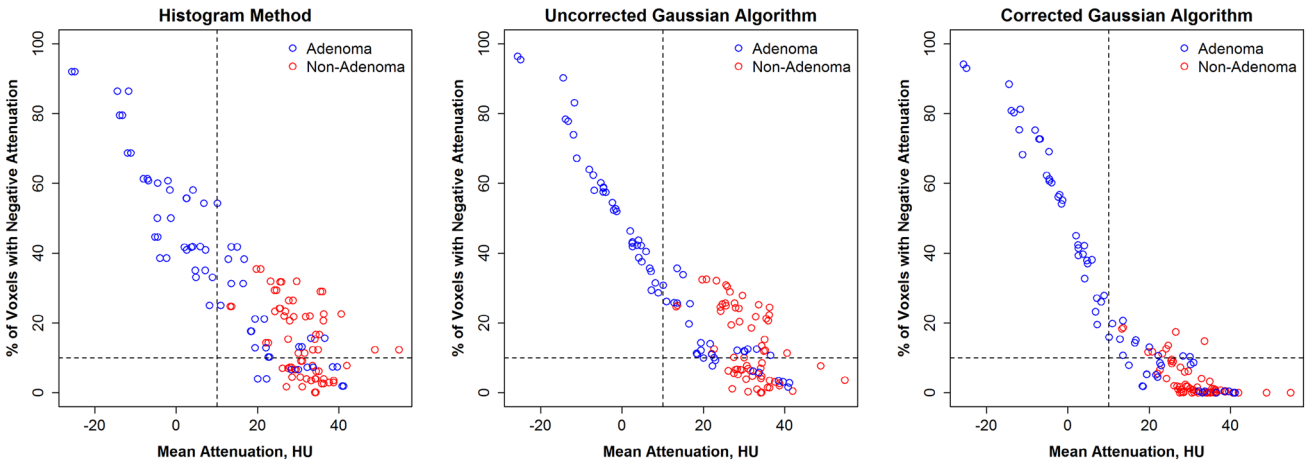

Fig. 4 Relationships between mean attenuation and percent of voxels with negative attenuation based on three methods. Blue and red points denote adenomas and non-adenomas, respectively. The vertical dashed line indicates the 10 HU threshold used for mean attenuation, and the horizontal dashed line indicates the 10% threshold for the other methods

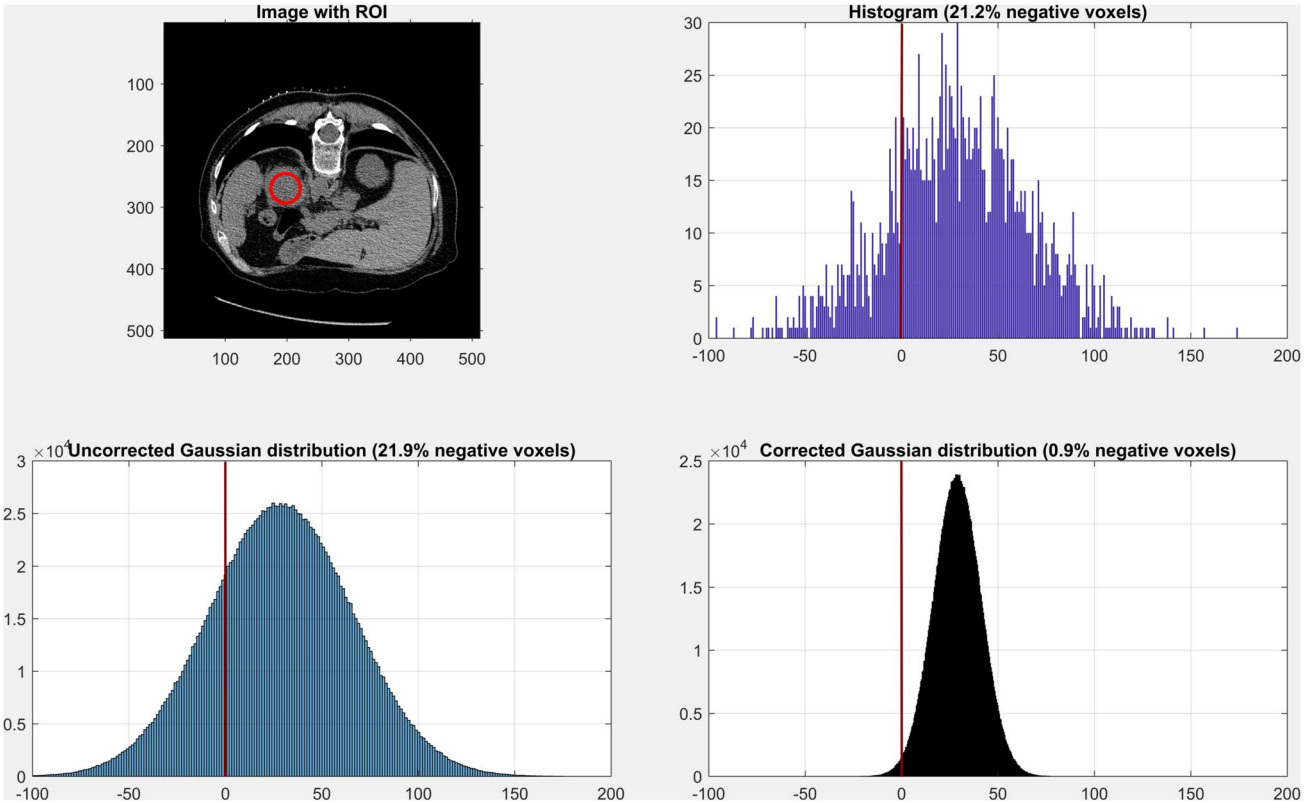

Fig. 5 67-year-old woman with bilateral adrenal nodules biopsy-proven to be lung cancer metastases. Study acquired in helical mode with slice thickness 2.5 mm, mA 120, rotation time 0.5 s, and pitch 1.375. Mean attenuation of the left-sided nodule was 28.8 HU with an uncorrected standard deviation of 37.2 HU and corrected standard deviation of 12.3 HU. Histogram analysis shows 21.2% negative attenuation voxels; uncorrected Gaussian algorithm shows 21.9% negative attenuation voxels; and corrected Gaussian algorithm shows 0.9% negative attenuation voxels. This represents a false positive for adenoma by the histogram and uncorrected Gaussian algorithm methods, and a true negative for adenoma by the corrected Gaussian algorithm and mean attenuation method

attenuation method. Figure 6 shows a different patient with a pathology-proven lung cancer metastasis that was false positive for adenoma by all methods except mean attenuation.

Discussion

Although the mean attenuation method has been shown to have high specificity in characterizing adrenal nodules, it is known to have difficulty identifying lipid-poor adenomas. The histogram method initially showed increased sensitivity in identifying more of these lipid-poor adenomas while maintaining specificity; however it is unclear if this technique is still a valid option given more recent CT acquisition parameters resulting in increased image noise [5]. Our study demonstrates that use of histogram analysis with modern imaging parameters will result in excessive false-positive classification of non-adenomas as adenomas (on average 19 malignant lesions misclassified as adenomas by the histogram method and 18 by the uncorrected Gaussian) resulting in low specificity of 42–47% in adenoma classification for both the histogram method and uncorrected Gaussian algorithm.

Lin and colleagues have recognized that the specificity of histogram analysis is low in noisy images and have suggested a workaround of rejecting data with a standard deviation threshold > 30 HU [14]. In our data, we find that 25.7% of the adrenal nodules have standard deviations of 30 HU or greater—throwing out these data would result in a large de facto decrease in sensitivity. In addition, this histogram method frequently still requires post processing at a separate work station, which can impede work flow. Our study demonstrates a faster and more accurate method to analyze the negative pixels within a ROI, with the additional benefit of incorporating noise correction via the corrected Gaussian algorithm. The Gaussian algorithm with noise correction utilizes mean attenuation, standard deviation, effective mAs, and reconstructive slice thickness, which are readily available on PACS. Although some PACS implement histogram analysis natively, most do not offer its functionality. In contrast, the Gaussian algorithm method can be performed without having to use a separate work station as the data

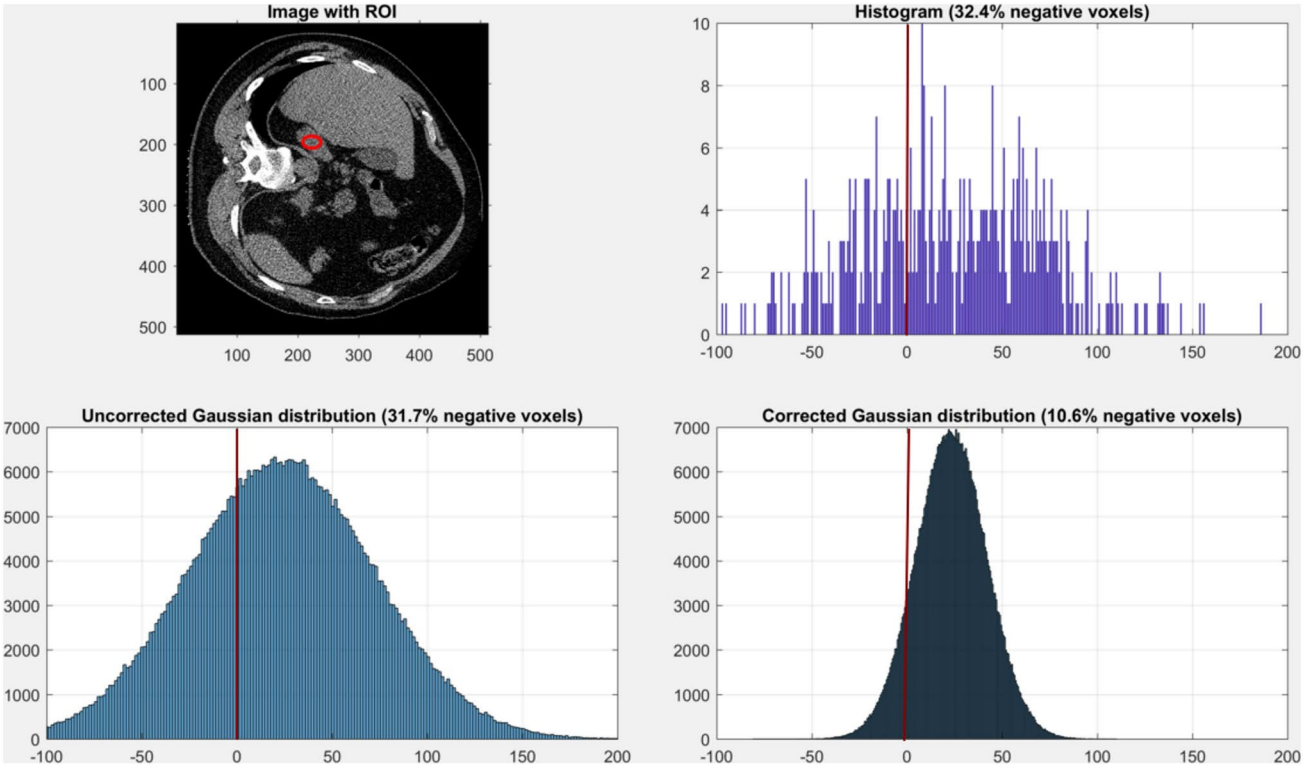

Fig. 6 54-year-old man with bilateral adrenal nodules proven pathologically to be lung cancer metastases. Study acquired in helical mode with slice thickness 2.5 mm, mA 100, rotation time 0.8 s, and pitch 1.375. Mean attenuation of the left-sided nodule was 24.9 HU with an uncorrected standard deviation of 54.6 HU and corrected standard deviation of 20.8 HU. Histogram analysis shows 32.4% negative attenuation voxels; uncorrected Gaussian algorithm shows 31.7% negative attenuation voxels; and corrected Gaussian algorithm shows 10.6% negative attenuation voxels. This represents a false positive for adenoma by histogram, uncorrected Gaussian algorithm, and corrected Gaussian algorithm methods, but a true negative by mean attenuation

obtained by drawing a ROI on any standard PACS can be easily inputted into the Open Source web application that we developed.

Our data showed low absolute specificity for both the histogram method and the uncorrected Gaussian, indicating a high rate of non-adenomas being falsely diagnosed as adenomas. As a result, these non-noise-corrected methods should not be applied to modern day CT studies. After applying noise correction to the histogram-analog Gaussian algorithm, specificity was significantly improved, albeit not to 100%. This is not unexpected, as prior studies of the histogram method demonstrated less than 100% specificity (range of 88–100%) [5–10]. However, this may limit its applicability in patients with known malignancy where the probability of metastasis is higher.

After noise correction, the corrected Gaussian algorithm and the mean attenuation method had similar overall accuracy, and the mean attenuation method still demonstrated significantly greater specificity when using the commonly employed threshold of 10 HU. The 100% specificity of mean attenuation method in our data set may reflect sampling bias, as prior studies have shown the existence of non-adenomas with mean attenuation below < 10 HU [12]. Our data show no convincing rationale for using the histogram method or uncorrected Gaussian algorithm, due to their low absolute specificity.

Nevertheless, our study's use of noise correction may have implications outside of adrenal adenoma categorization, as characterization methods that utilize CT should either be independent from image noise or incorporate noise correction in their construction. This is relevant for CT texture analysis techniques, whose measures of standard deviation, kurtosis, gray-level uniformity, and entropy could all be susceptible to image-noise differences [15, 16].

Our study has a few notable limitations. It relies on the use of noncontrast CT images, which are not always available. It was performed with retrospectively collected image data from a single institution, which may limit its generalizability, especially given the number of cases gathered and our size restriction to nodules equal to or greater than 14 mm diameter. Not all cases of adenomas were confirmed via biopsy, although our methodology for classification is consistent with extant literature [2, 5, 6, 10, 12]. There may exist sampling bias, as our retrospective methods of free-text

query and correlation with a biopsy database may not have returned all the cases that truly existed. The incidence of malignancies in the non-adenoma dataset may confound results, as certain malignancies (e.g. hepatocellular carcinoma and clear cell renal cell carcinoma) may inherently result in lower attenuation metastases due to their cellular composition. The heterogeneity of CT techniques employed is a limitation, as the effects of image noise may be different in boundary cases such as the very low-dose technique often employed during CT-guided biopsies. This is reflected in the significantly lower mAs, mA, and uncorrected standard deviation of Hounsfield unit measurements for the non-adenoma subgroup as compared to the adenoma subgroup. However, the noise-corrected standard deviation was not significantly different, further demonstrating the effectiveness of the noise correction method. Future work should include evaluating the performance of this noise-corrected Gaussian method for the indeterminate adrenal nodules measuring greater than 10 Hounsfield units on noncontrast CT to determine if the algorithm can help identify more adenomas and thus obviate further work up.

In conclusion, characterization of adrenal nodules as adenomas or non-adenomas has high clinical relevance. With modern low-dose CT technique the specificity of the histogram method for discrimination of adrenal adenomas and non-adenomas is lower than with previous higher dose scans. The specificity and accuracy of a histogram-equivalent method can be increased mathematically through image noise correction, and the corrected Gaussian algorithm has improved sensitivity to the mean attenuation with similar accuracy albeit with lower specificity. Although this suggests limited utility for histogram analysis in adrenal nodule characterization, our study demonstrates the potential mathematical application for other noise dependent CT characterization methods.

Compliance with ethical standards

Conflict of interest One of the authors, Mr. Hippe, has several research grants to disclose: Research Grant, Koninklijke Philips NV; Research Grant, General Electric Company; Research Grant, Toshiba America Medical Systems. These grants did not support this study. None of the other authors have financial disclosures or conflicts of interest to declare.

Ethical approval The institutional review board at University of Washington Medical Center approved this study.

References

1. Song JH, Chaudhry FS, Mayo-Smith WW (2008) The incidental adrenal mass on CT: prevalence of adrenal disease in 1,049 consecutive adrenal masses in patients with no known malignancy. AJR Am J Roentgenol 190:1163-8.
2. Lee MJ, Hahn PF, Papanicolaou N, et al. (1991) Benign and malignant adrenal masses: CT distinction with attenuation coefficients, size, and observer analysis. Radiology 179:415-8.
3. Caoili EM, Korobkin M, Francis IR, et al. (2002) Adrenal masses: characterization with combined unenhanced and delayed enhanced CT. Radiology 222:629-33.
4. Boland GW, Blake MA, Hahn PF, Mayo-Smith WW (2008) Incidental adrenal lesions: principles, techniques, and algorithms for imaging characterization. Radiology 249:756-75.
5. Bae KT, Fuangtharnthip P, Prasad SR, Joe BN, Heiken JP (2003) Adrenal masses: CT characterization with histogram analysis method. Radiology 228:735-42.
6. Jhaveri KS, Wong F, Ghai S, Haider MA (2006) Comparison of CT histogram analysis and chemical shift MRI in the characterization of indeterminate adrenal nodules. AJR Am J Roentgenol 187:1303-8.
7. Jhaveri KS, Wong F, Ghai S, Haider MA (2006) Comparison of CT histogram analysis and chemical shift MRI in the characterization of indeterminate adrenal nodules. AJR Am J Roentgenol 187:1303-8.
8. Remer EM, Motta-Ramirez GA, Shepardson LB, Hamrahian AH, Herts BR (2006) CT Histogram Analysis in Pathologically Proven Adrenal Masses. American Journal of Roentgenology 187:191-6.
9. Perri M, Erba P, Volterrani D, et al. (2011) Adrenal Masses in Patients With Cancer: PET/CT Characterization With Combined CT Histogram and Standardized Uptake Value PET Analysis. American Journal of Roentgenology 197:209-16.
10. Ho LM, Paulson EK, Brady MJ, Wong TZ, Schindera ST (2008) Lipid-poor adenomas on unenhanced CT: does histogram analysis increase sensitivity compared with a mean attenuation threshold? AJR Am J Roentgenol 191:234-8.
11. Power SP, Moloney F, Twomey M, James K, O'Connor OJ, Maher MM (2016) Computed tomography and patient risk: Facts, perceptions and uncertainties. World journal of radiology 8:902-15.
12. Hsu LD, Wang CL, Clark TJ Characterization of Adrenal Adenoma by Gaussian Model-Based Algorithm. Current problems in diagnostic radiology 45:312-8.
13. Rocha TO, Albuquerque TC, Nather JC, Jr., et al. (2018) Histogram Analysis of Adrenal Lesions With a Single Measurement for 10th Percentile: Feasibility and Incremental Value for Diagnosing Adenomas. AJR Am J Roentgenol 211:1227-33.
14. Lin MF, Chang-Sen LQ, Heiken JP, Pilgram TK, Bae KT (2015) Histogram analysis for characterization of indeterminate adrenal nodules on noncontrast CT. Abdominal imaging 40:1666-74.
15. Lubner MG, Smith AD, Sandrasegaran K, Sahani DV, Pickhardt PJ (2017) CT Texture Analysis: Definitions, Applications, Biologic Correlates, and Challenges. Radiographics : a review publication of the Radiological Society of North America, Inc 37:1483-503.
16. Lubner MG, Stabo N, Abel EJ, Del Rio AM, Pickhardt PJ (2016) CT Textural Analysis of Large Primary Renal Cell Carcinomas: Pretreatment Tumor Heterogeneity Correlates With Histologic Findings and Clinical Outcomes. AJR Am J Roentgenol 207:96-105.

Affiliations

Toshimasa J. Clark[1] · Larson D. Hsu[2] · Daniel Hippe[3] · Sophie Cowan[3] · Jonathan Carnell[3] · Carolyn L. Wang[3]

Larson D. Hsu
larsonhsu@gmail.com

Daniel Hippe
dhippe@uw.edu

Sophie Cowan
smcowan@uw.edu

Jonathan Carnell
carnell1@uw.edu

Carolyn L. Wang
wangcl@uw.edu

[1] Abdominal Imaging Division, Department of Radiology, University of Colorado Denver, Anschutz Medical Campus, 12401 E 17th Ave, Mail Stop L954, Aurora, CO 80045, USA

[2] Department of Radiology, Roswell Park Cancer Institute, Body Imaging Section Elm & Carlton Streets, Buffalo, NY 14263, USA

[3] Body Imaging Section, Department of Radiology, University of Washington, Box 358081, 825 Eastlake Ave E, G2-600, Seattle, WA 98109, USA